Contents lists available at SciOpen

Food Science and Human Wellness

journal homepage: https://www.sciopen.com/journal/2097-0765

China Food Publishing Co.

De novo production of lacto-*N*-neotetraose by metabolic engineering of *Saccharomyces cerevisiae* as a cell factory

Han Liu[a,b,c], Yingjie Liu[a,b,c], Haitao Hu[a,b,c], Chenlu Zhu[a,b,c], Shuang Zhang[a], Xiaomei Lyu [a,b,c,*], Ruijin Yang[a,b,c,*]

[a] State Key Laboratory of Food Science and Resources, Jiangnan University, Wuxi 214122, China
[b] School of Food Science and Technology, Jiangnan University, Wuxi 214122, China
[c] Collaborative Innovation Center of Food Safety and Quality Control in Jiangsu Province, Jiangnan University, Wuxi 214122, China

ARTICLE INFO

Article history:
Received 8 December 2023
Received in revised form 31 January 2024
Accepted 5 July 2024

Keywords:
Lacto-*N*-neotetraose
Saccharomyces cerevisiae
GAL system
Modular engineering

ABSTRACT

Lacto-*N*-neotetraose (LNnT) is a crucial neutral core human milk oligosaccharide (HMO). In this study, we established a LNnT-producing *Saccharomyces cerevisiae* cell factory through comprehensive metabolic engineering. Specifically, the *de novo* biosynthetic pathway of LNnT was assembled by heterologously expressing the lactose permease (*lac12*) from *Kluyveromyces lactis* and the glycosyltransferase from *Neisseria meningitidis* in *S. cerevisiae*. Subsequently, carbon source regulation based on the glucose-sensitive GAL regulatory system was employed to optimize the expression time of heterologous genes, achieving a production of 15.61 mg/L of LNnT in shake-flask fermentation. In addition, the key rate-limiting steps involved in LNnT synthesis pathway were identified and the corresponding genes were overexpressed to enhance LNnT production, resulting in an 8-fold increase in LNnT titer compared to that of parental strain. To our knowledge, this is the first report on LNnT biosynthesis in *S. cerevisiae*, opening up the possibility of green production of LNnT using food-safe microorganisms.

1. Introduction

Human milk oligosaccharides (HMOs) are the third most abundant solid constituent of human milk after lactose and lipids. HMOs play a crucial role in breastfeeding infants by regulating intestinal flora, developing the immune system, preventing necrotizing enterocolitis and improving brain development and cognitive ability[1-5]. HMOs can be categorized into 3 primary groups based on their attached monomers: 1) fucosylated neutral HMOs, 2) sialylated acidic HMOs, and 3) non-fucosylated neutral HMOs[6-7]. Among them, neutral HMOs account for over 75% of all HMOs present in breast milk. Lacto-*N*-neotetraose (LNnT), an essential non-fucosylated neutral HMO, has diverse biological functions such as enhancing the immune system, regulating intestinal flora, promoting cell maturation, and accelerating wound healing[8-10]. It also serves as a glycoantigen associated with tumors and has garnered significant attention for its potential applications in nutrition and pharmaceuticals. Furthermore, LNnT is the second additive after 2′-fucosyllactose (2′-FL) approved by the European Food Safety Authority (EFSA) and the U.S. Food and Drug Administration (FDA) for addition to milk powder and beverages[11-12].

The World Health Organization strongly advocates for exclusive breastfeeding during the first 6 months of an infant's life due to its numerous health benefits[13]. Nevertheless, personal, sociocultural, and economic factors often impede this goal. Currently, only 38% of infants worldwide are exclusively breastfed. The infant formula industry has seen a substantial increase in sales, exceeding 40% in

* Corresponding authors at: State Key Laboratory of Food Science and Resources, Jiangnan University, Wuxi 214122, China.
E-mail address: xmlyu@jiangnan.edu.cn (X.M. Lyu); yrj@jiangnan.edu.cn (R.J Yang)
Peer review under responsibility of Beijing Academy of Food Sciences.

SciOpen Publishing services by Tsinghua University Press

http://doi.org/10.26599/FSHW.2024.9250342

recent years[14]. As for the production of LNnT, 4 different approaches have been adopted: isolation from human milk, chemical synthesis, enzymatic synthesis and microbiological fermentation. However, human milk sources are limited, and chemical synthesis involves a multi-step process that is costly and complex[15]. Enzymatic synthesis requires active enzymes from microbial sources and expensive intermediates under stringent conditions[16]. By contrast, microbial biosynthesis of LNnT is more cost-effective and scalable than other methods.

In recent decades, LNnT has been successfully synthesized by microorganisms such as *Escherichia coli*[17-21] and *Bacillus subtilis*[22-23]. Various strategies have been employed to enhance LNnT production, including CRISPRi-guided multiplexed fine-tuning of metabolic flux[22], optimizing heterologous enzyme expression and reducing competing pathway metabolic fluxes[18], improving lactose utilization and metabolic pathway optimization[17] among others. Although significant advancements have been made in LNnT production by both *E. coli* and *B. subtilis*, its production by *Saccharomyces cerevisiae* remains unreported. Recognized as Generally Recognized as Safe (GRAS), *S. cerevisiae* has been used in food for thousands of years and offers advantages over bacteria such as no endotoxins or spore issues and reduced susceptibility to phage contamination during fermentation. Therefore, *S. cerevisiae* may be ideal for manufacturing food and cosmetic ingredients due to its excellent properties.

In this study, we developed an alternative approach for producing LNnT by engineering a GRAS strain, *S. cerevisiae*, through *de novo* pathway construction and multi-module regulation (Fig. 1). To ensure lactose absorption, lactose permease (*lac12*) from *Kluyveromyces lactis* was introduced into *S. cerevisiae*. A *de novo* synthetic pathway of LNnT was then constructed by assembling heterologous *β*-1,3-*N*-acetylglucosamine aminotransferase (*lgtA*), *β*-1,4-galactosyltransferase (*lgtB*), and *lac12* into the genome of the host strain BY4741. We verified the production ability using mass spectrometry. Furthermore, we optimized the LNnT synthesis pathway through carbon source modulation based on the glucose-sensitive GAL regulatory system and multi-module engineering to increase LNnT titer. This study represents the first exploration of using *S. cerevisiae* as a platform to produce LNnT.

2. Materials and methods

2.1 Strains, culture conditions and reagents

E. coli DH5α was used for recombinant DNA manipulation and plasmid construction. All the *E. coli* strains were cultured in Luria-Bertani (LB) medium, contained 10 g/L tryptone, 5 g/L yeast extract and 10 g/L NaCl. When necessary, the culture medium was supplemented with 50 μg/mL kanamycin (Kan) or 100 μg/mL ampicillin (Amp).

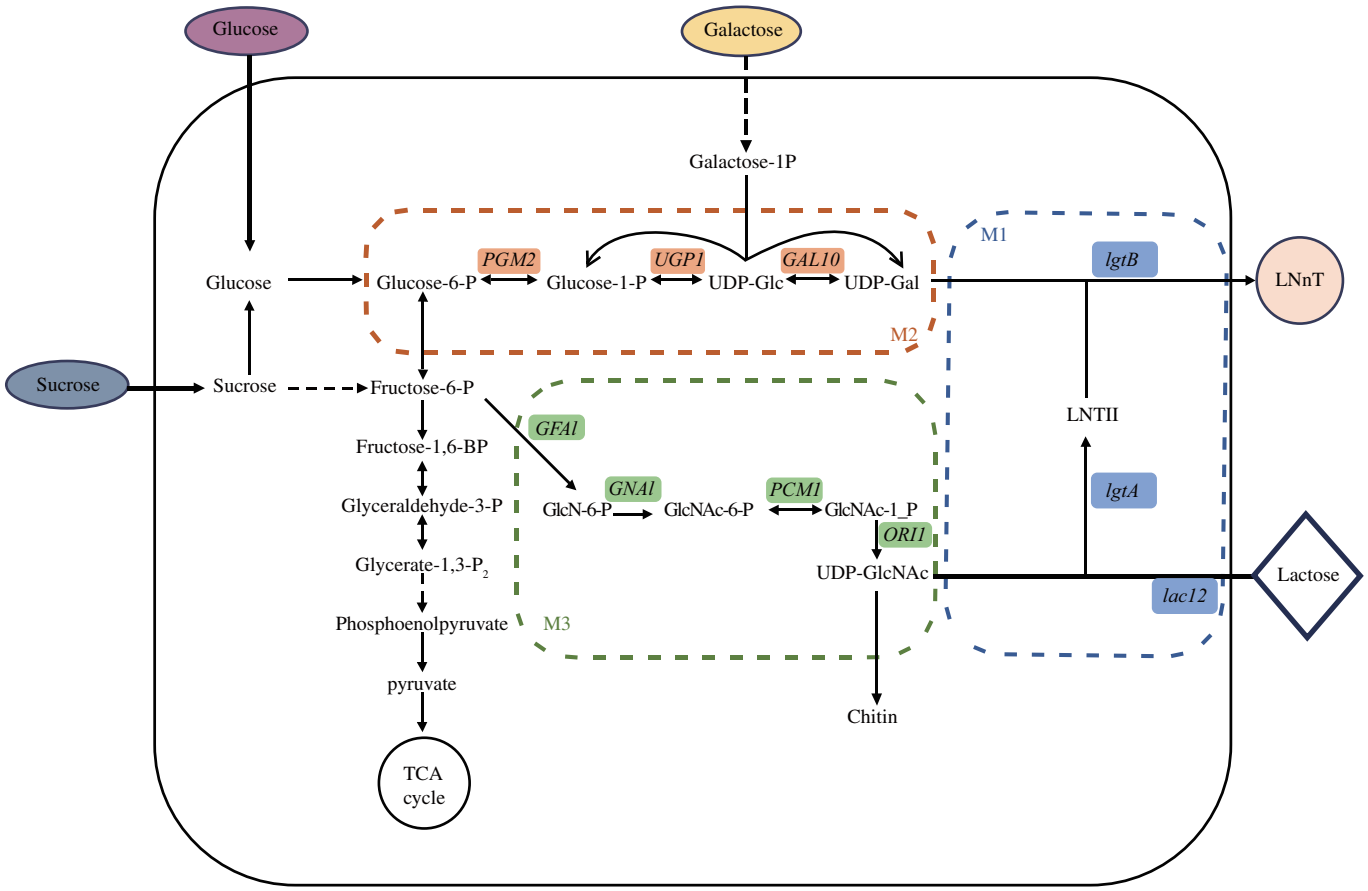

Fig. 1 Schematic diagram for *de novo* production of LNnT by metabolic engineering of *S. cerevisiae via* multi-module regulation. M1 (module 1): heterologous pathway containing *lac12*, *lgtA* and *lgtB*; M2 (module 2): *PGM2*, *UGP1* and *GAL10*; M3 (module 3): *GFA1*, *GNA1*, *PCM1* and *QRI1*. UDP-Glc, uridine 5'-diphospho-glucose; GlcNAc-1-P, *N*-acetylglucosamine-1-phosphate; GlcNAc-6-P, *N*-acetylglucosamine-6-phosphate; GlcN-6-P, glucosamine-6-phosphate; TCA cycle, tricarboxylic acid cycle.

The yeast BY4741 strain, derived from *S. cerevisiae* S288C, served as the host for LNnT biosynthesis. The engineered *S. cerevisiae* constructed in this study are listed in Tables 1 and S4. We used various media for culturing, including Yeast extract Peptone Dextrose medium (YPD medium: 20 g/L tryptone, 20 g/L dextrose, 10 g/L yeast extract), YPS medium (20 g/L tryptone, 20 g/L sucrose, 10 g/L yeast extract), YPG medium (20 g/L tryptone, 20 g/L galactose, 10 g/L yeast extract) and SCG medium (Synthetic Complete drop-out medium with 20 g/L galactose, 1.7 g/L yeast nitrogen base, 5 g/L anhydrous ammonium sulfate, 100 mL/L 10 × total amino acids) containing 200 μg/mL geneticin (G418) or 40 μg/mL bleomycin (Ble) for culturing *S. cerevisiae* carrying plasmids pCEV-G1-Km, pUMRI or pCEV-G1-Ph. We used SD-FOA medium (1.7 g/L yeast nitrogen base without amino acids, 5 g/L anhydrous ammonium sulfate, 100 mL/L 10× dropout solution, and 2 g/L glucose with 0.1% (*m*/*V*) 5-fluoroorotic acid) for selecting yeast transformants with KanMX-URA-PRB322ori marker excision.

The antibiotics were purchased from Titan Scientific (Shanghai, China) and Sangon Biotechnology (Shanghai, China). Molecular biology kits and reagents were obtained from TianGen Biotechnology (Beijing, China) and Takara Biotechnology (Dalian, China). The media components utilised in this study were procured from Sangon Biotechnology (Shanghai, China). The LNnT chemical standard was obtained from Huicheng Biotechnology (Shanghai, China). Additional chemical reagents were acquired from Coolaber (Beijing, China).

Table 1
Strains used in this study.

Strains	Parental strain	Description	Source
BY4741	S288C	*MATa*, *his3*Δ1, *leu2*Δ0, *met15*Δ0, *ura3*Δ0	[31]
YLH-4L	BY4741	BY4741 harboring plasmids pCEV-G1-Ph-GAL1,10-*lac12*^{opt} and pCEV-G1-Km-*lac4*^{opt}	This study
BY-LGFP	BY4741	BY4741 harboring plasmids pCEV-G1-Ph-GAL1,10-*lac12*^{opt}-GFP	This study
YLH-10	BY4741	BY4741 in which the linearized pUMRI-B-ΔGAL80-*lgtA*^{opt}-*lgtB*^{opt} (P_{GAL7}-*lgtA*^{opt}-T_{TPS1}/P_{GAL2}-*lgtB*^{opt} -T_{PGK1}) have been integrated GAL80 locus	This study
YLH-11	YLH-10	BY4741 in which the linearized pUMRI-B-ΔGAL80-*lgtA*^{opt}-*lgtB*^{opt} and pUMRI-A-ΔHO-*lac12*^{opt} (P_{GAL7}-*lgtA*^{opt} -T_{TPS1}/ P_{GAL2}-*lgtB*^{opt} -T_{PGK1}, $P_{GAL1,10}$-*lac12*^{opt} -T_{CYC1}) have been integrated GAL80 and HO locus	This study
YLH-14	YLH-11	YLH-11 harboring plasmid pCEV-G1-Km-GAL1,10-*lgtA*^{opt}	This study
YLH-15	YLH-11	YLH-11 harboring plasmid pCEV-G1-Km-GAL1,10-*lgtB*^{opt}	This study
YLH-16	YLH-11	YLH-11 harboring plasmid pCEV-G1-Ph-GAL1,10-*lac12*^{opt}	This study
YLH-17	YLH-11	YLH-11 harboring plasmids pCEV-G1-Km-GAL1,10-*lgtA*^{opt} and pCEV-G1-Ph-GAL1,10-*lac12*^{opt}	This study
YLH-18	YLH-11	YLH-11 harboring plasmids pCEV-G1-Km-GAL1,10-*lgtB*^{opt} and pCEV-G1-Ph-GAL1,10-*lac12*^{opt}	This study
YLH-19	YLH-11	YLH-11 harboring plasmid pCEV-G1-Km-GAL1,10-*lgtA*^{opt}-*lgtB*^{opt}	This study
YLH-20	YLH-11	YLH-11 harboring plasmids pCEV-G1-Km-GAL1,10-*lgtA*^{opt}-*lgtB*^{opt} and pCEV-G1-Ph-GAL1,10-*lac12*^{opt}	This study
YLH-16-01	YLH-16	YLH-16 harboring plasmid pCEV-G1-Km-PGM2	This study
YLH-16-02	YLH-16	YLH-16 harboring plasmid pCEV-G1-Km-UGP1	This study
YLH-16-03	YLH-16	YLH-16 harboring plasmid pCEV-G1-Km-GAL10	This study
YLH-16-05	YLH-16	YLH-16 harboring plasmid pCEV-G1-Km-GFA1	This study
YLH-16-06	YLH-16	YLH-16 harboring plasmid pCEV-G1-Km-GNA1	This study
YLH-16-07	YLH-16	YLH-16 harboring plasmid pCEV-G1-Km-PCM1	This study
YLH-16-08	YLH-16	YLH-16 harboring plasmid pCEV-G1-Km-QRI1	This study
YLH-81	YLH-16	YLH-16 in which the linearized pUMRI-A-ΔDPP1-PGM2 (P_{GAL1}-*PGM2*-T_{TADH1}) have been integrated DPP1 locus	This study
YLH-82	YLH-16	YLH-16 in which the linearized pUMRI-A-ΔDPP1-GAL10 (P_{GAL1}-*GAL10*-T_{TADH1}) have been integrated DPP1 locus	This study
YLH-83	YLH-16	YLH-16 in which the linearized pUMRI-A-ΔDPP1-GFA1 (P_{GAL1}-*GFA1*-T_{TADH1}) have been integrated DPP1 locus	This study
YLH-84	YLH-16	YLH-16 in which the linearized pUMRI-A-ΔDPP1-GNA1 (P_{GAL1}-*GNA1* -T_{TADH1}) have been integrated DPP1 locus	This study
YLH-85	YLH-16	YLH-16 in which the linearized pUMRI-A-ΔDPP1-PCM1 (P_{GAL1}-*PCM1* -T_{TADH1}) have been integrated DPP1 locus	This study
YLH-86	YLH-16	YLH-16 in which the linearized pUMRI-A-ΔDPP1-QRI1 (P_{GAL1}-*QRI1* -T_{TADH1}) have been integrated DPP1 locus	This study

2.2 Plasmid construction

All plasmids referred to in this study and all primers used to construct plasmids are listed in Tables S1 and S2, respectively. The *β*-1,3-*N*-acetylglucosamine aminotransferase (*lgtA,* GenBank ID: 904226, listed in Table S3) and *β*-1,4-galactosyltransferase (*lgtB*, GenBank ID: 904227, listed in Table S3) are derived from *Neisseria meningitidis* MC58. The lactose permease (*lac12,* GenBank ID: 2897085, listed in Table S3) and *β*-galactosidase (*lac4*, GenBank ID: 2897170, listed in Table S3) are derived from *K. lactis*. All gene sequences were codon-optimized and synthesized by Sangon Biotechnology (Shanghai, China) and GeneScript (Suzhou, China). The synthesized *lgtA* gene fragment was inserted into pUMRI-B-ΔGAL80 and pCEV-G1-Km-GAL vectors at *Bam*HI/*Sal*I sites, resulting in pUMRI-B-ΔGAL80-*lgtA*^{opt} and pCEV-G1-Km-GAL-*lgtA*^{opt}. The codon-optimized *lgtB* gene was inserted between the *Eco*RI/*Not*I sites of pCEV-G1-Km-GAL vector to obtain pCEV-G1-Km-GAL-*lgtB*^{opt}. The *lgtA* and *lgtB* gene fragments were cloned sequentially into the pUMRI-B-ΔGAL80 or pCEV-G1-Km-GAL vector to generate either pUMRI-B-ΔGAL80-*lgtA*^{opt}-*lgtB*^{opt} plasmid or pCEV-G1-Km-GAL-*lgtA*^{opt}-*lgtB*^{opt} plasmid. For the construction of plasmid pUMRI-A-ΔHO-*lac12*^{opt}, the *lac12* gene was subcloned between the *Bam*HI/*Sal*I sites of the pUMRI-A-ΔHO vector. The codon-optimized *lac4* gene was subcloned into plasmid pCEV-G1-Km at *Sal*I/*Nhe*I sites, yielding plasmid pCEV-G1-Km-*lac4*^{opt}. All recombinant vectors have been validated by Sangon Biotechnology (Shanghai, China), Generic (Suzhou, China) and Gencefe Biotech (Wuxi, China). The endogenous target enzymes involved in uridine diphosphate galactose (UDP-Gal) and uridine diphosphate *N*-acetylglucosamine (UDP-GlcNAc) synthesis pathway, such as phosphoglucomutase (PGM2), UDP-glucose pyrophosphorylase (UGP1), UDP-glucose epimerase (GAL10), fructose-6-phosphate transaminase (GFA1), glucosamine 6-phosphate *N*-acetyltransferase (GNA1), phosphoacetylglucosamine mutase (PCM1) and UDP-*N*-acetylglucosamine diphosphorylase (QRI1) (Table S3), were amplified from *S. cerevisiae* BY4741 genome using primer pairs listed in Table S2. These amplified genes were later inserted at *Not*I/*Spe*I sites of the pCEV-G1-Km vector to create recombinant plasmids pCEV-G1-Km-PGM2, pCEV-G1-Km-UGP1, pCEV-G1-Km-GAL10, pCEV-G1-Km-GFA1, pCEV-G1-Km-GNA1, pCEV-G1-Km-PCM1 and pCEV-G1-Km-QRI1. The *PGM2, GAL10*, *GFA1*, *GNA1*, *PCM1* and *QRI1* gene fragment was inserted into pUMRI-21-ΔDPP1 vector at *Not*I/*Spe*I or *Not*I/*Pac*I sites, resulting in pUMRI-21-ΔDPP1-PGM2, pUMRI-21-ΔDPP1-GAL10, pUMRI-21-ΔDPP1-GFA1, pUMRI-21-ΔDPP1-GNA1, pUMRI-21-ΔDPP1-PCM1 and pUMRI-21-ΔDPP1-QRI1.

2.3 Construction of engineered S. cerevisiae

All the strains used in this study are detailed in Table 1. Plasmids of pCEV-G1-Ph-GAL1,10-*lac12*^{opt} and pCEV-G1-Km-*lac4*^{opt} were transformed into *S. cerevisiae* BY4741 to generate BY4741-L4 strain. The biosynthetic pathway of LNnT was assembled by co-expression of the *lac12*, *lgtA* and *lgtB* genes in *S. cerevisiae* BY4741. Specifically, plasmids of pUMRI-B-ΔGAL80-*lgtA*^{opt}-*lgtB*^{opt} and pUMRI-A-ΔHO-*lac12*^{opt} were sequentially linearized by the restriction enzyme *Sfi*I and then integrated into the genome of *S. cerevisiae* BY4741 through electroporation transformation, resulting in the engineered strain YLH-11. The chromosomal integration steps were performed according to the procedures described in a previous study[24].

To obtain engineered strains YLH-14, YLH-15, YLH-16, YLH-17, YLH-18, YLH-19 and YLH-20 for optimizing the heterologous LNnT pathway, plasmids pCEV-G1-Km-GAL1,10-*lgtA*^{opt}, pCEV-G1-Km-GAL1,10-*lgtB*^{opt}, pCEV-G1-Ph-GAL1,10-*lac12*^{opt}, pCEV-G1-Km-GAL1,10-*lgtA*^{opt}/pCEV-G1-Ph-GAL1,10-*lac12*^{opt}, pCEV-G1-Km-GAL1,10-*lgtB*^{opt}/pCEV-G1-Ph-GAL1,10-*lac12*^{opt} and pCEV-G1-Km-GAL1,10-*lgtA*^{opt}-*lgtB*^{opt}/pCEV-G1-Ph-GAL1,10-*lac12*^{opt} were transformed into the engineered strain YLH-11 respectively.

To obtain the engineered strains YLH-16-01, YLH-16-02, YLH-16-03, YLH-16-05, YLH-16-06, YLH-16-07, YLH-16-08 for optimizing UDP-Gal and UDP-GlcNAc biosynthetic pathway, plasmids pCEV-G1-Km-*PGM2*, pCEV-G1-Km-*UGP1*, pCEV-G1-Km-*GAL10*, pCEV-G1-Km-*GFA1*, pCEV-G1-Km-*GNA1*, pCEV-G1-Km-*PCM1* and pCEV-G1-Km-*QRI1* were transformed into the strain YLH-16 respectively.

To obtain the engineered strains YLH-81, YLH-82, YLH-83, YLH-84, YLH-85 and YLH-86, plasmids pUMRI-21-ΔDPP1-*PGM2*, pUMRI-21-ΔDPP1-*GAL10*, pUMRI-21-ΔDPP1-*GFA1*, pUMRI-21-ΔDPP1-*GNA1*, pUMRI-21-ΔDPP1-*PCM1* and pUMRI-21-ΔDPP1-*QRI1* were sequentially linearized by the restriction enzyme *Sfi*I and then integrated into the genome of engineered *S. cerevisiae* YLH-16 through electroporation transformation.

2.4 Shake-flask fermentation

The microbial synthesis of LNnT was performed by shake-flask fermentation using the engineered strains. For LNnT production, the engineered yeasts were initially pre-cultured in 5 mL of YPD medium with the appropriate antibiotic concentration overnight at 30 °C and 220 r/min. The cells in mid-exponential phase were harvested, washed with sterile water, and then transferred to 20 mL of SDG medium, YPS medium, YPD medium or YPG medium (including 2 g/L lactose) containing suitable antibiotics in 100 mL flasks. They were incubated under similar conditions for 96 h.

2.5 Determination of dry cell weight

To determine the dry cell weights (DCW) of the engineered yeast strains, 4 mL of culture broth was centrifuged at 10 000 × *g* for 10 min and washed twice with sterile water. After removing the water through centrifugation, the cells were dried to a constant weight at 95 °C.

2.6 Quantitative real-time PCR

A single yeast colony was inoculated into YPD medium and cultured until it reached the logarithmic growth phase as a seed solution. The cells were then inoculated into different media (YPD, YPS, YPG) for fermentation. RNA was extracted using the total RNA extraction Kit (TaKara, Dalian, China) at different fermentation times, and reverse transcribed into cDNA using the PrimeScript™ RT reagent kit with gDNA Eraser (TaKara). Quantitative PCR (qPCR) was conducted using the TB Green® *Premix Ex Taq*™ II FAST qPCR (TaKara) on a LightCycler 480 II *real-time* PCR instrument (Roche Applied Science). The internal reference gene was *ACT1*, and the transcription levels of related genes were determined using the $2^{-\Delta\Delta Ct}$ method.

2.7 Analytic methods

2.7.1 Detection of concentrations of LNnT

To ascertain the concentrations of LNnT in engineered *S. cerevisiae*, appropriate amounts of culture broth were centrifuged at 10 000 × *g* for 10 min. Subsequently, the supernatant and pellet were collected independently to determine extracellular and intracellular LNnT concentrations. Prior to analysis, the supernatant was deproteinated using the sevage method[25-26] and filtered through a 0.22 μm hydrophilic membrane for extracellular LNnT assays. The pellet was washed twice, resuspended in an equal volume of sterile water, then ground with steel balls for 300 s. After centrifugation, the supernatant was deproteinated and filtered through the membrane for intracellular LNnT concentration determination.

2.7.2 LNnT biosynthesis analysis

To confirm LNnT biosynthesis, LNnT standard and samples fermented by engineered strains were analyzed using a Sciex LC coupled to an AB Sciex 5500 triple quadrupole trap mass spectrometer (Q-TRAP-MS) with electrospray ionization (ESI) in positive mode. The unit (Waters) was equipped with a Waters ACQUITY UPLC BEH Amide column (2.1 mm × 100 mm, 1.7 μm). The column was eluted at a flow rate of 0.3 mL/min at 40 °C with gradients in mobile phase A (0.1% (*V*/*V*) formic acid) and B (100% (*V*/*V*) acetonitrile). The mobile phase gradient shifted from 5% A/95% B to 60% A/40% B over 11 min. Compound-dependent parameters for standard compounds were optimized by direct infusion on the mass spectrometer to achieve maximum multiple reaction monitoring (MRM) signal intensities. General instrument parameters such as gas settings, heat settings, and ion spray voltage were optimized for all compounds by flow injection analysis (FIA) using ultra-performance liquid chromatography (UPLC) flow rates. These instrument parameters were set to a common value suitable for all compounds within a single run period. Instrument control and data integration were performed using Analyst Software Version 1.6.2. LNnT content was expressed as milligrams per gram of dry cell weight (mg/g DCW) and milligrams per liter of fermentation broth (mg/L)[27].

2.7.3 Cell density analysis

Cell density, measured at 600 nm ($OD_{600\ nm}$), was monitored with a spectrophotometer. The concentrations of galactose, sucrose, glucose and lactose were measured using a Waters high-performance liquid chromatography (HPLC) 1200 series system equipped with a Rezex ROA-Organic Acid H+ (8%) column (Phenomenex, Torrance, CA, USA) and a refractive index detector. The column was eluted with 0.005 mol/L H_2SO_4 at a flow rate of 0.6 mL/min at 50 °C. The content of LNnT was expressed as previously described.

2.8 Data analysis

The yield data of LNnT were analyzed using Analyst Software (version 1.6.2). All experiments were repeated at least 3 times independently, and the statistical analyses were performed using one-way analysis of variance.

3. Results and discussion

3.1 De novo synthesis of LNnT in engineered S. cerevisiae

The synthesis of LNnT in *S. cerevisiae* was achieved using intracellular UDP-GlcNAc and UDP-Gal as precursors, supplemented with lactose as a substrate. Initially, heterologously expressed *β*-1,3-*N*-acetylglucosamine aminotransferase catalyzed the generation of Lacto-*N*-triose II (LNTII) from UDP-GlcNAc and lactose. Subsequently, LNTII and UDP-Gal were catalyzed by heterologously expressed *β*-1,4-galactosyltransferase to produce LNnT.

3.1.1 Functional validation of lactose permease Lac12

As *S. cerevisiae* cannot naturally assimilate lactose, an essential precursor for the synthesis of LNnT (Fig. 2A), a heterologous lactose permease must be introduced to construct the LNnT synthetic pathway. In this study, the *lac12* gene encoding lactose permease from *K. lactis* was introduced into the *S. cerevisiae* BY4741 strain. To ensure successful expression and accurate localization of the *lac12* gene on the membrane of *S. cerevisiae*, the *lac12* gene carrying green fluorescent protein (GFP) was introduced into BY4741 to obtain the engineered strain BY-LGFP, and its expression was observed by laser scanning confocal microscopy (LSCM). As shown in Fig. 2B, lactose permease Lac12 was successfully expressed in yeast and correctly localized on the membrane. To evaluate the functional expression of Lac12 in *S. cerevisiae*, we measured the extracellular lactose concentrations of the engineered strain YLH-4L, expressing both lactose permease and *β*-galactosidase, as well as the parent strain-BY4741, after incubating with 2 g/L lactose for 18 h. As displayed in Fig. 2C, the extracellular lactose concentration of the YLH-4L strain decreased significantly compared to BY4741. However, the $OD_{600\ nm}$ of YLH-4L was much lower than that of BY4741 due to the high metabolic stress caused by the introduction of dual plasmids.

3.1.2 Construction of the de eovo synthetic pathway of LNnT in S. cerevisiae

Inspired by previous studies on LNnT biosynthesis[23], LgtA and LgtB from *N. meningitidis* MC58 were selected for introduction into the yeast genome along with the *lac12* gene to construct the complete synthetic pathway of LNnT (Fig. 1), generating the engineered strain YLH-11 (Fig. 3A). The Q-TRAP-MS results of fermentation broth samples from engineered strain YLH-11 showed that compounds in the fermentation samples had the same mass spectra as the LNnT standard (Fig. 3B), confirming that engineered *S. cerevisiae* YLH-11 could synthesize LNnT. Meanwhile, the LC profiles in Fig. 3B indicated that the parent strain BY4741 could not produce LNnT, demonstrating that the *de novo* synthesis pathway for LNnT was successfully constructed in *S. cerevisiae.*

3.2 Enhancing LNnT synthesis via carbon source regulation based on GAL System

In light of the competitive relationship between LNnT synthesis and *S. cerevisiae* growth (Fig. 1), this study selected the GAL system to control gene expression timing to improve LNnT production[28]. In *S. cerevisiae*, GAL promoters are activated by GAL4 transcription

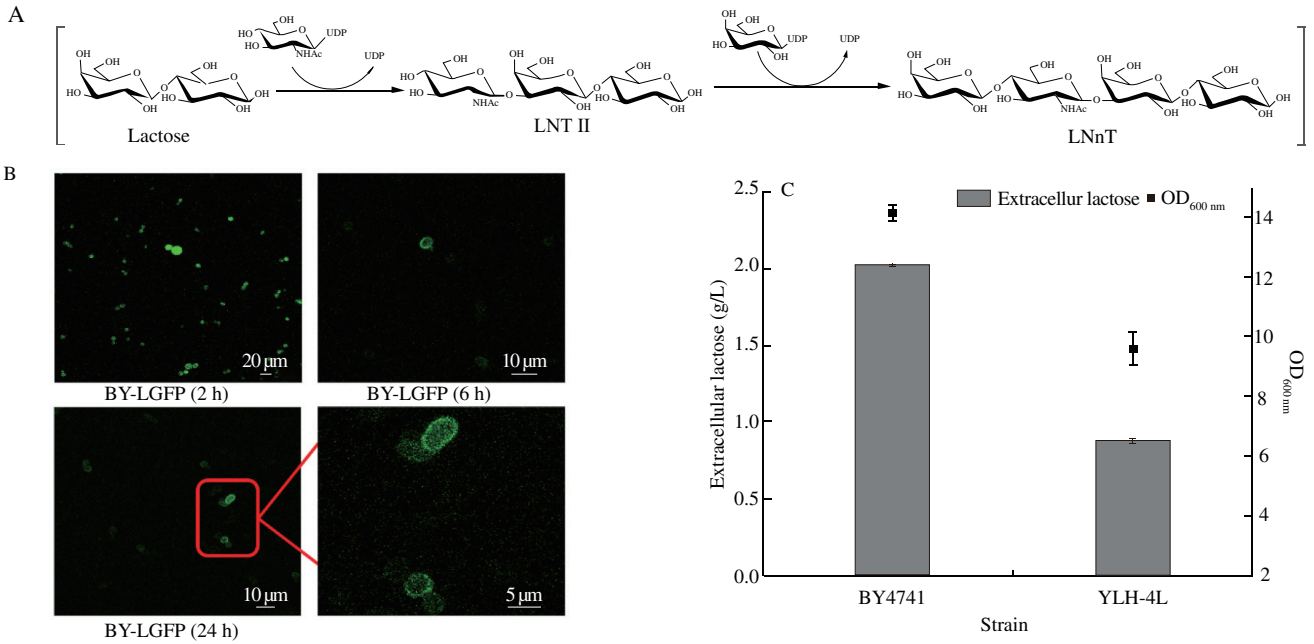

Fig. 2 Process for LNnT synthesis from lactose and functional validation of Lac12. (A) Steps of LNnT synthesis deficient in *S. cerevisiae*. (B) Expression and localization of Lac12 at different fermentation times. (C) Comparison of lactose utilization by parental strain BY4741 and engineered *S. cerevisiae* YLH-4L.

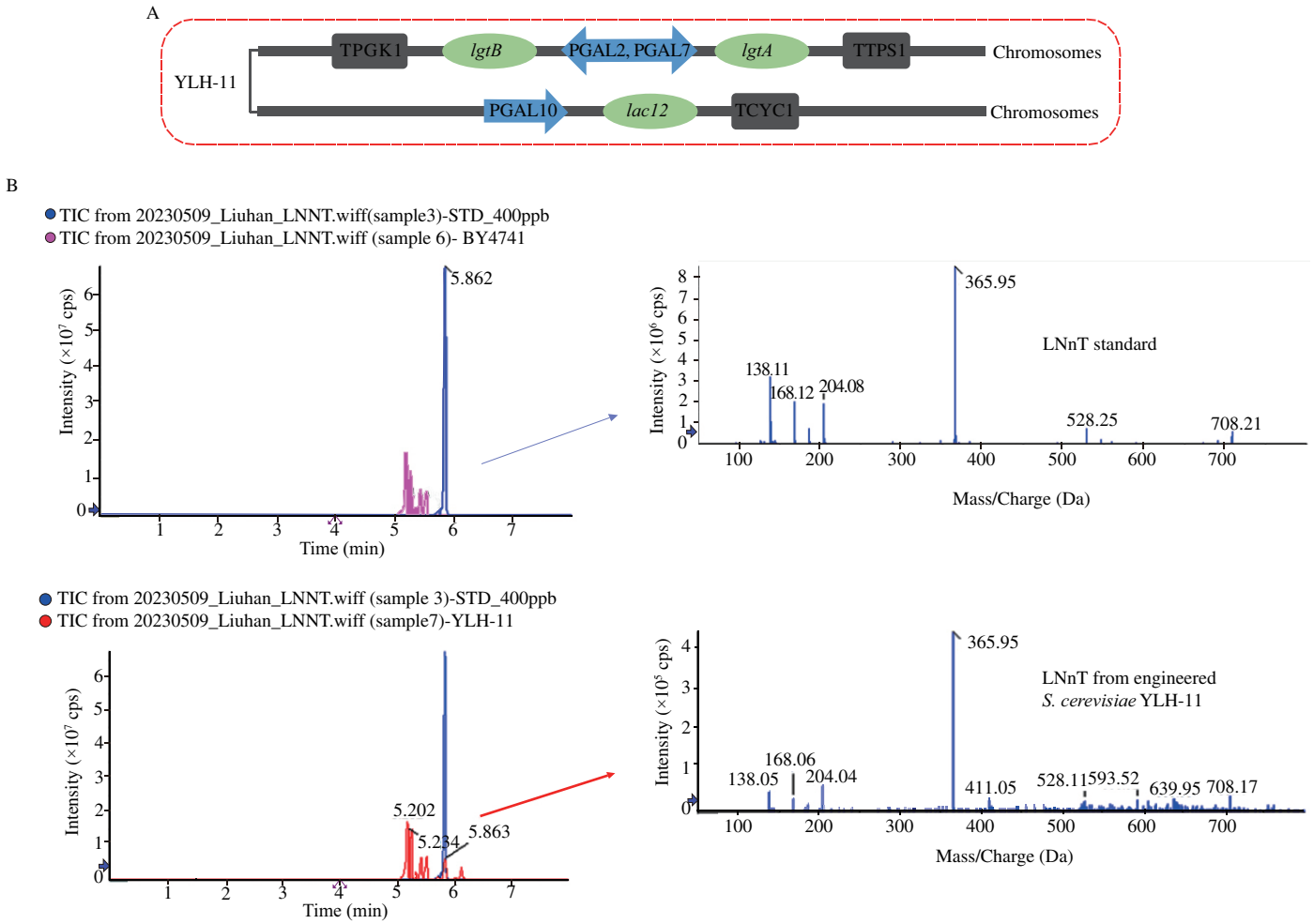

Fig. 3 Confirmation of LNnT synthesis in engineered *S. cerevisiae* YLH-11 by LC-MS. (A) The engineered *S. cerevisiae* YLH-11 integrating the *de novo* LNnT synthetic pathway into the genome. (B) LC-MS profile of the wild-type strain-BY4741 (the upper profile, in purple) and YLH-11 (the lower profile, in red), using LNnT standard as the control (in blue).

factor binding; P_{GAL4} is dual-regulated by glucose and galactose: when galactose is present, it stimulates *GAL3p* expression, which represses GAL80p expression, allowing *GAL4p* to active GAL promoter; without galactose, GAL80p binds to Gal4p, preventing activation of GAL promoters (Fig. 4A). When glucose is used as a carbon source, high concentrations inhibit *Snf1p* expression, releasing Mig1p to repress P_{GAL4}, thereby inhibiting GAL promoter, low glucose concentration cause *Snf1p* to repress *Mig1p*, activating GAL promoters[24, 27]. An inducer-free carbon source regulatory system was established by knocking out *GAL80*, allowing direct regulation of GAL promoters by glucose concentration, which high concentrations inhibit gene expression, while low concentrations initiate it.

In our previous investigation, we established a glucose-sensitive GAL regulatory system based on *GAL80* knockout to dynamically regulate isoprenoids in yeast, which yielded promising results[24,29-30]. In this study, this set of system was utilized to dynamically regulate the expression of the key genes, *lgtA*, *lgtB*, and *lac12*. Additionally, we designed glucose-limited media (YPS, with 2% sucrose; YPD, with 2% glucose; and YPG, with 2% galactose) to control gene expression timing for LNnT production, effectively regulating LNnT yield (Fig. 4B). In this phase, sucrose, glucose and galactose were used as the sole carbon source, respectively, for fermenting of engineered *S. cerevisiae* YLH-11. The LNnT titer of YLH-11 reached 6.80 mg/L with sucrose as the carbon source. With glucose as the sole carbon source, a larger proportion was allocated to strain growth during the initial fermentation stage due to higher glucose concentration. Moreover, genes for LNnT production were activated when glucose levels decreased, resulting in a shorter expression duration than with sucrose and a yield of 3.50 mg/L LNnT. When galactose was used, the engineered yeast produced LNnT while growing, and gene expression duration was the longest.

To verify the hypothesis, we investigated carbon source consumption and gene expression levels regulated by GAL system at different fermentation times, using 48 h as a reference point. The results, shown in Fig. 5, confirmed that the GAL system is sugar-responsive, albeit with some early leakage. Nevertheless, it is evident that gene expression levels are relatively high with galactose as the carbon source, followed by sucrose and glucose.

The results of carbon source regulation are depicted in Figs. 4B-E. The engineered yeast YLH-11 with galactose as the sole carbon source outperformed the other two carbon sources in LNnT/LNTII production, achieving 15.61 mg/L LNnT (comprising 14.65 mg/L extracellular and 0.95 mg/L intracellular LNnT). These results also indicated that nearly 93% of the LNnT produced was effectively expelled from the yeast cells.

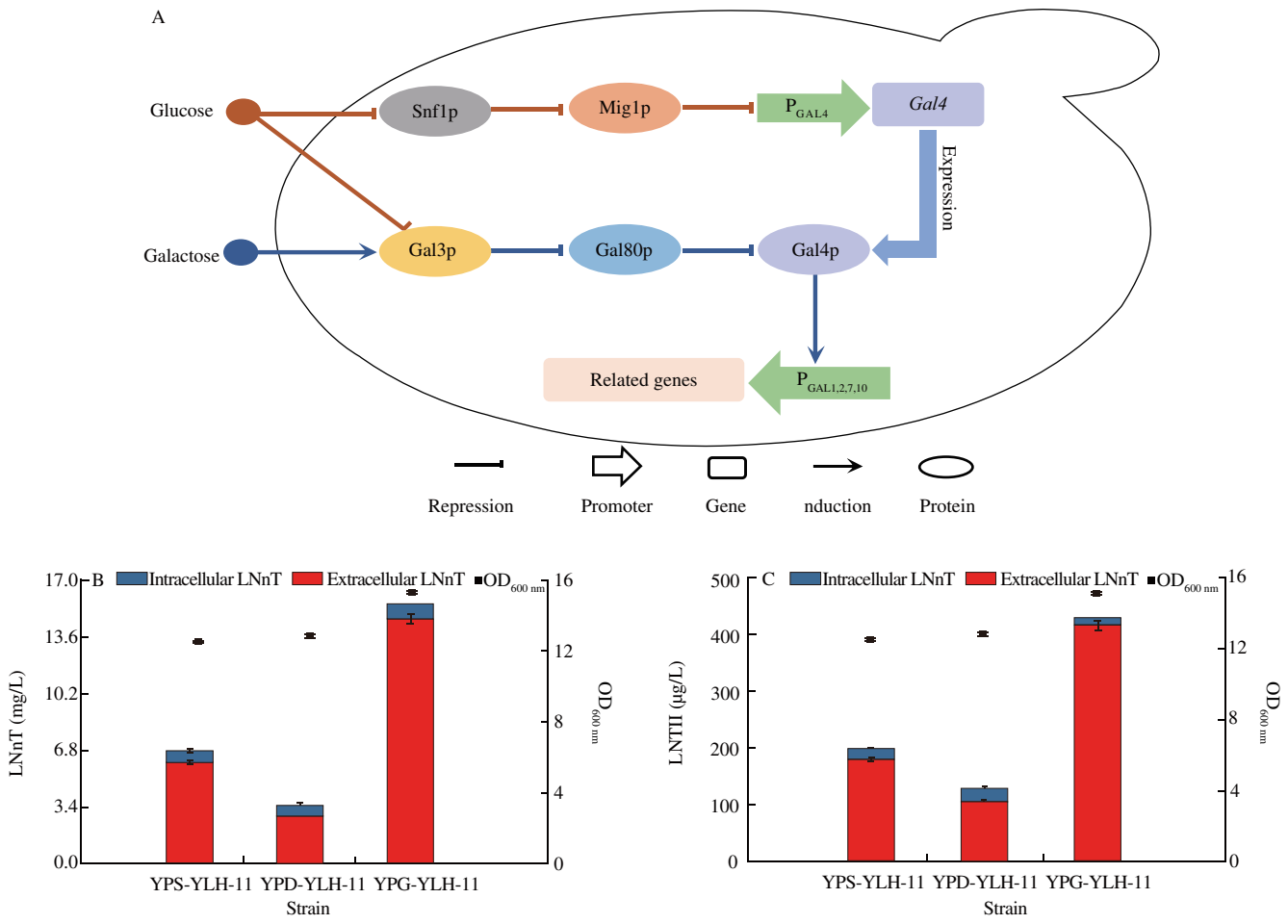

Fig. 4 Effects of different carbon sources on LNnT production of engineered *S. cerevisiae*. (A) Schematic of the GAL regulated system in *S. cerevisiae*. (B) LNnT titer and $OD_{600\ nm}$ values of engineered *S. cerevisiae* YLH-11 in different media. (C) LNTII titer and $OD_{600\ nm}$ values of engineered *S. cerevisiae* YLH-11 in different media. (D) LNnT production and DCW of engineered *S. cerevisiae* YLH-11 in different media. (E) LNTII production and DCW of engineered *S. cerevisiae* YLH-11 in different media. Other abbreviations: YPS-YLH-11, *S. cerevisiae* YLH-11 fermented with YPS medium; YPD-YLH-11, *S. cerevisiae* YLH-11 fermented with YPD medium; YPG-YLH-11, *S. cerevisiae* YLH-11 fermented with YPG medium.

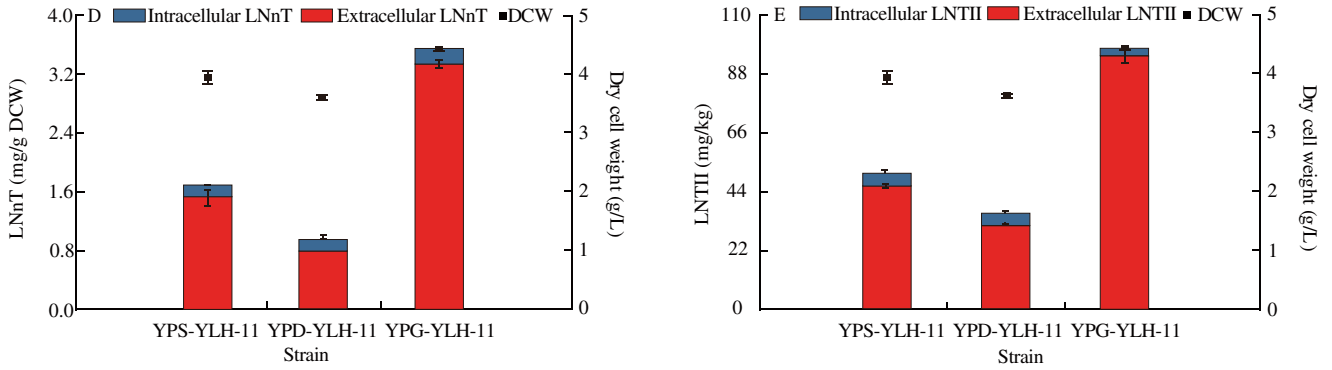

Fig. 4 (*Continued*)

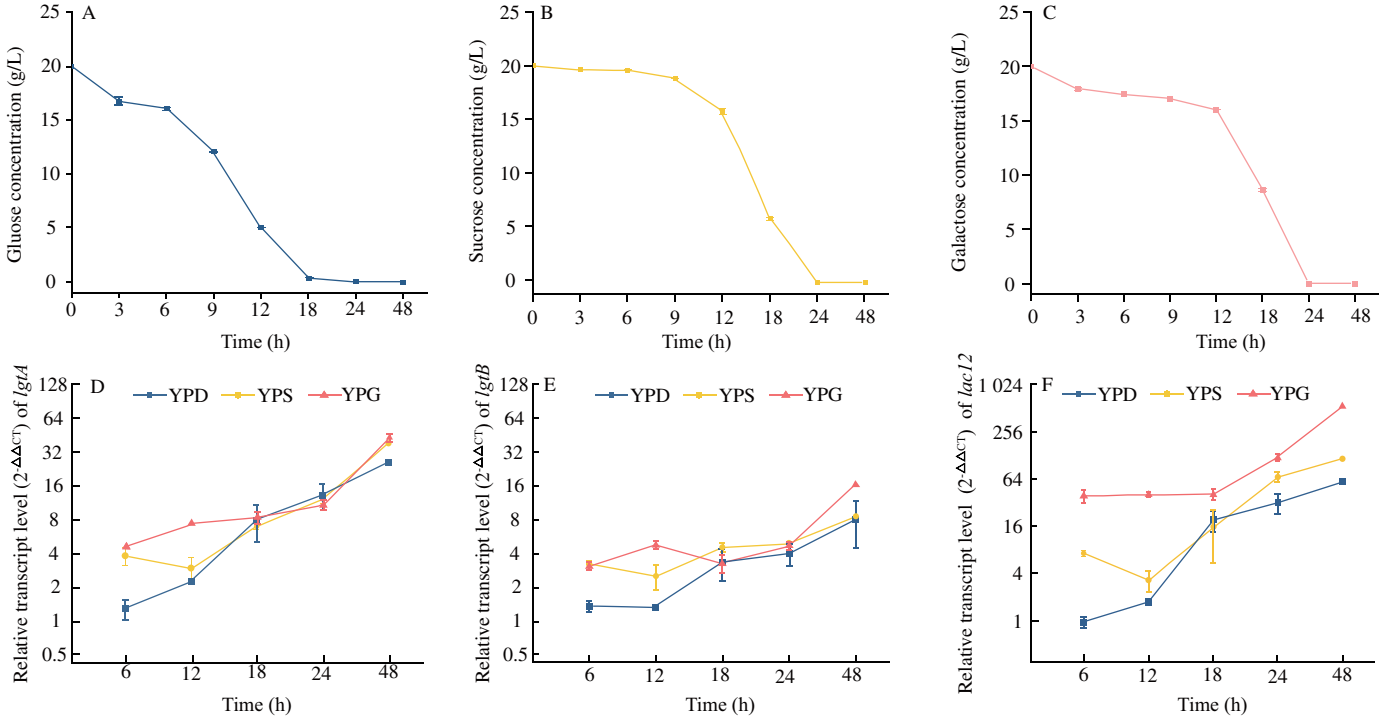

Fig. 5 Consumption of carbon sources and expression levels of heterologous genes at different fermentation times. (A) Glucose consumption curve during fermentation of the engineered yeast YLH-11 using YPD as fermentation medium. (B) Sucrose consumption curve during fermentation of the engineered yeast YLH-11 using YPS as fermentation medium. (C) Galactose consumption curve during fermentation of the engineered yeast YLH-11 using YPG as fermentation medium. (D) Relative transcript levels of *lgtA* under different carbon sources with different fermentation times. (E) Relative transcript levels of *lgtB* under different carbon sources with different fermentation times. (F) Relative transcript levels of *lac12* under different carbon sources with different fermentation times.

3.3 Improvement of LNnT synthesis through multi-module engineering

Although we achieved *de novo* biosynthetic pathway expression of *lac12* from *K. lactis* and *lgtA* and *lgtB* from *N. meningitidis*, the LNnT yield remained low. We hypothesized that rate-limiting steps within the metabolic pathway impeded efficient LNnT synthesis. To increase precursor molecule availability and eliminate rate-limiting steps, we employed a multi-module engineering approach by dividing the LNnT synthesis pathway into 3 modules for regulation: the heterologous synthesis module (M1), the UDP-Gal supply module (M2), and the UDP-GlcNAc supply module (M3) (Fig. 1).

3.3.1 Module 1-the LNnT heterologous synthetic module

In module 1, 7 engineered *S. cerevisiae* strains, including YLH-14, YLH-15, YLH-16, YLH-17, YLH-18, YLH-19 and YLH-20, were constructed by overexpressing heterologous genes (*lgtA*, *lgtB*, and *lac12*) in plasmid form using engineered *S. cerevisiae* YLH-11 as the parental strain (Fig. 6A). This was done to explore pivotal enzymes involved in the heterologous pathway of LNnT production.

The results demonstrated that the growth of the strains was negatively affected to differing extents by the overexpression of heterologous genes in the form of plasmids, resulting in reduced biomass. The $OD_{600\ nm}$ of the parental strain YLH-11 was about 15, while the $OD_{600\ nm}$ of the engineered strains YLH-14, YLH-15, YLH-16, YLH-17, YLH-18, YLH-19, YLH-20 decreased to about 11, 8, 7, 10, 8 after the addition of the plasmids with the overexpressed genes. However, in terms of the yields of intermediate LNTII and end product LNnT, the engineered yeast with heightened expression of the heterologous genes showed improved yields to varying extents. The extracellular LNnT production of YLH-14, YLH-15, YLH-16, YLH-17, YLH-18, YLH-19, and YLH-20 reached approximately 26, 18, 46,

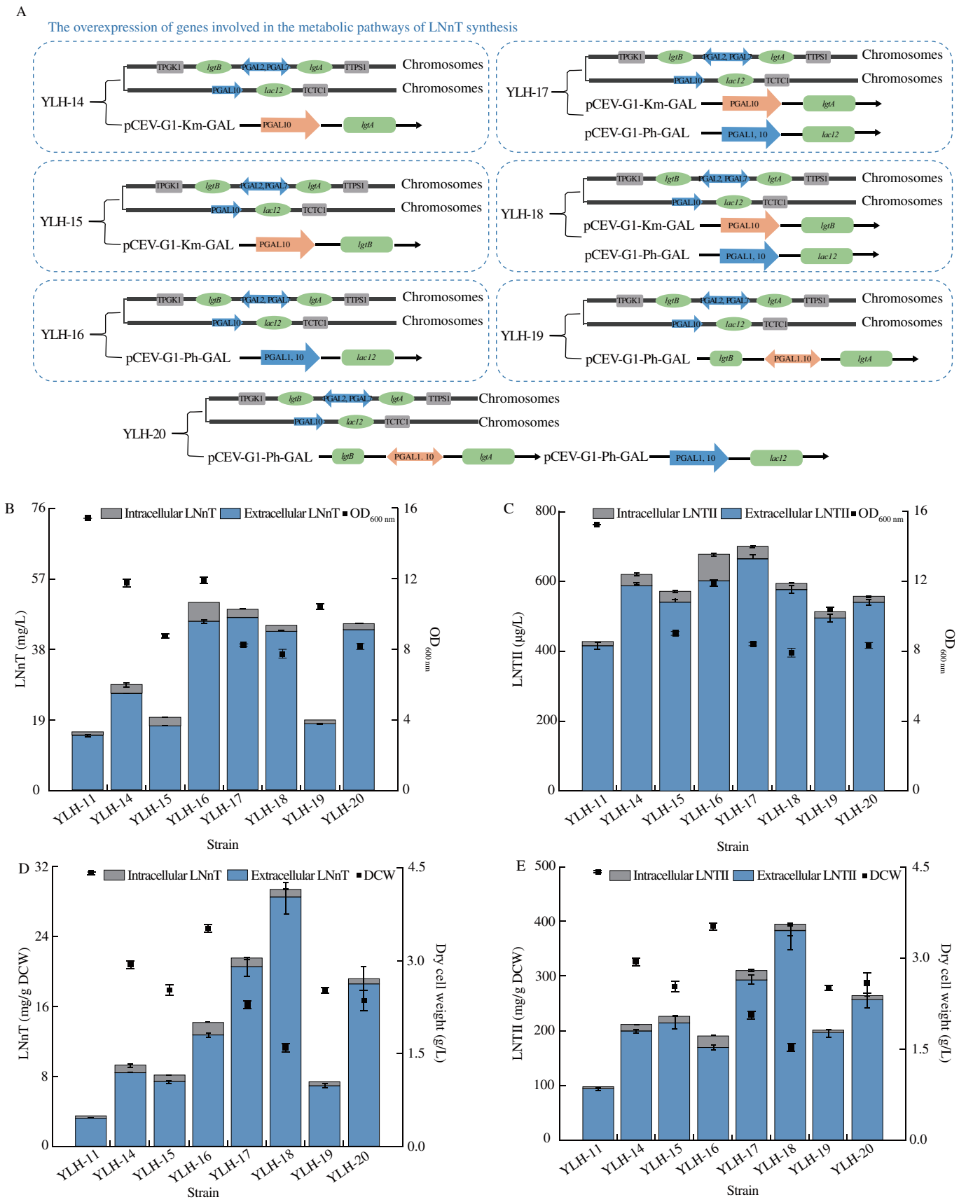

Fig. 6 Comparison of LNnT production in the engineered *S. cerevisiae* with module 1 regulation. (A) *S. cerevisiae* involved in module 1 and their characterization (all strains were based on YLH-11). (B) LC-MS analysis of LNnT synthesis of engineered *S. cerevisiae* YLH-11, YLH-14, YLH-15, YLH-16, YLH-17, YLH-18, YLH-19, YLH-20. (C) LC-MS analysis of LNTII synthesis of the above engineered *S. cerevisiae.* (D) LNnT production and DCW of the above engineered *S. cerevisiae*. (E) LNTII production and DCW of the above engineered *S. cerevisiae*.

47, 43, 18 and 43 mg/L, respectively (Fig. 6). This result indicated that the 3 heterologous genes at this stage are all rate-limiting factors affecting LNnT synthesis, therefore, overexpression of any gene can yield positive results. Moreover, the yield of *S. cerevisiae* YLH-16 with augmented expression of the lactose permease Lac12 exhibited the most significant increase, reaching 50.61 mg/L (about 3.2-fold increase compared with that of *S. cerevisiae* YLH-11). However, the LNnT titer (Fig. 6A) of *S. cerevisiae* YLH-17, YLH-18 or YLH-20 overexpressing 2 or 3 heterologous genes at the same time was lower than that of *S. cerevisiae* YLH-16 expressing the heterologous *lac12* gene alone, which may be due to excessive metabolic stress (dry cell weight showed in Fig. 6D) from the two-plasmid system or insufficient Gal4 protein. Meanwhile, the LNnT titer of *S. cerevisiae* YLH-14, YLH-15 or YLH-19 compared to the other engineered yeasts indicated that the main rate-limiting step in the current stage of research lay within lactose permease deficiency. Because the engineered strains YLH-14, YLH-15, and YLH-19 overexpressing the 2 glycosyltransferases alone only achieved a modest enhancement in LNnT yield, whereas the engineered strain YLH-16 overexpressing the lactose permease alone demonstrated a marked increase in LNnT yield.

Furthermore, the results of LNnT production (Fig. 6D) showed that the LNnT production fermented by *S. cerevisiae* YLH-17, YLH-18 and YLH-20 was higher than that of *S. cerevisiae* YLH-16, reaching about 21, 29, and 19 mg/g DCW, respectively. The LNnT production fermented by *S. cerevisiae* YLH-16 was only about 13 mg/g DCW. These results indicated that glycosyltransferases LgtA and LgtB become the rate-limiting enzymes when the expression of lactose permease expression is sufficiently high. The results also revealed that the 2 glycosyltransferases currently used in LNnT production by *E. coli* and *B. subtilis* may not be suitable for *S. cerevisiae*. Nevertheless, glycosyltransferases are indispensable for LNnT biosynthesis in *S. cerevisiae*. Consequently, a series of screening procedures were conducted to identify an optimal glycosyltransferase for LNnT synthesis in *S. cerevisiae* (Fig. 7). Unfortunately, no other glycosyltransferases were found to be more suitable for LNnT biosynthesis in *S. cerevisiae*. Future research should delve deeper into exploring glycosyltransferase sources or employ directed evolution approaches to obtain an optimal glycosyltransferase for LNnT biosynthesis in yeast. Subsequent high-copy assembly may then represent an effective strategy to enhance LNnT production in yeast cell factories.

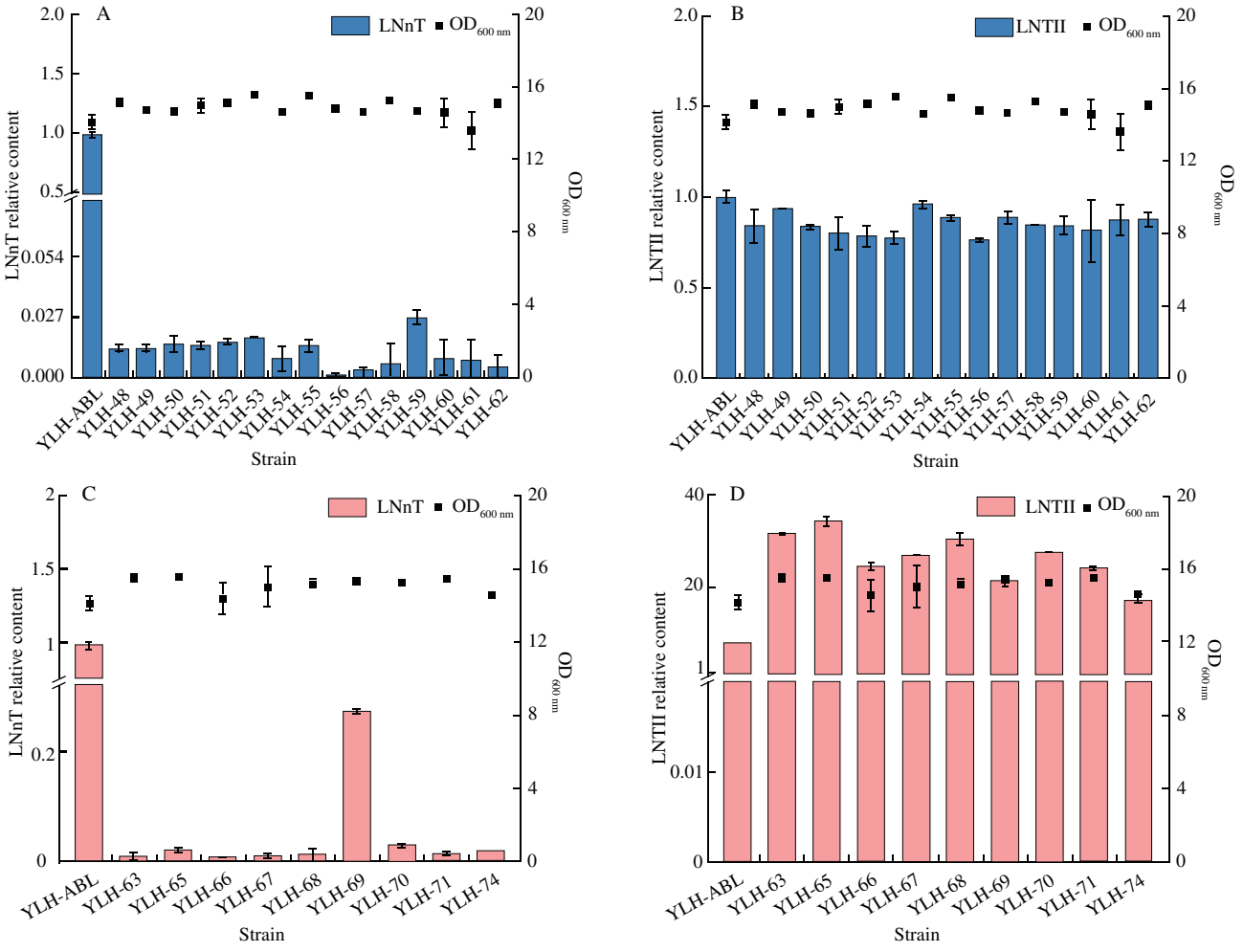

Fig. 7 Screening for heterologous glycosyltransferases in module 1. (A) LC-MS analysis of LNnT synthesis in engineered yeast carrying different *β*-1,3-*N*-acetylglucosamine aminotransferases. (B) LC-MS analysis of LNTII synthesis in engineered yeast carrying different *β*-1,3-*N*-acetylglucosamine aminotransferases. (C) LC-MS analysis of LNnT synthesis in engineered yeast carrying different *β*-1,4-galactosyltransferase. (D) LC-MS analysis of LNTII synthesis in engineered yeast carrying different *β*-1,4-galactosyltransferase.

3.3.2 *Module 2-the UDP-Gal supply module*

In module 2, 3 engineered *S. cerevisiae* strains (YLH-16-01, YLH-16-02 and YLH-16-03) were constructed to investigate key enzymes of UDP-Gal supply module by overexpressing endogenous genes *PGM2*, *UGP1* and *GAL10* in plasmid form using engineered yeast YLH-16 as the parental strain (Fig. 6A).

As shown in Fig.8, overexpression of endogenous genes likewise affected strain growth to varying degrees, likely due to metabolic stress caused by the strong promoter and dual plasmid system. Based on the titers of LNnT and LNTII depicted in bar graphs (Figs. 8B and C), no critical endogenous genes were identified. However, according to the yields of LNnT and LNTII shown in Figs. 8D and E, it is apparent that the fermentation production by *S. cerevisiae* YLH-16-01 (19.59 mg/g DCW) and YLH-16-03 (18.22 mg/g DCW) were significantly higher than that of the parental strain (14.33 mg/g DCW). This indicated that PGM2 and GAL10 were key enzymes for module 2. Therefore, further studies could focus on enhancing PGM2 and GAL10 expression enhancement at the genomic level to augment UDP-Gal supply.

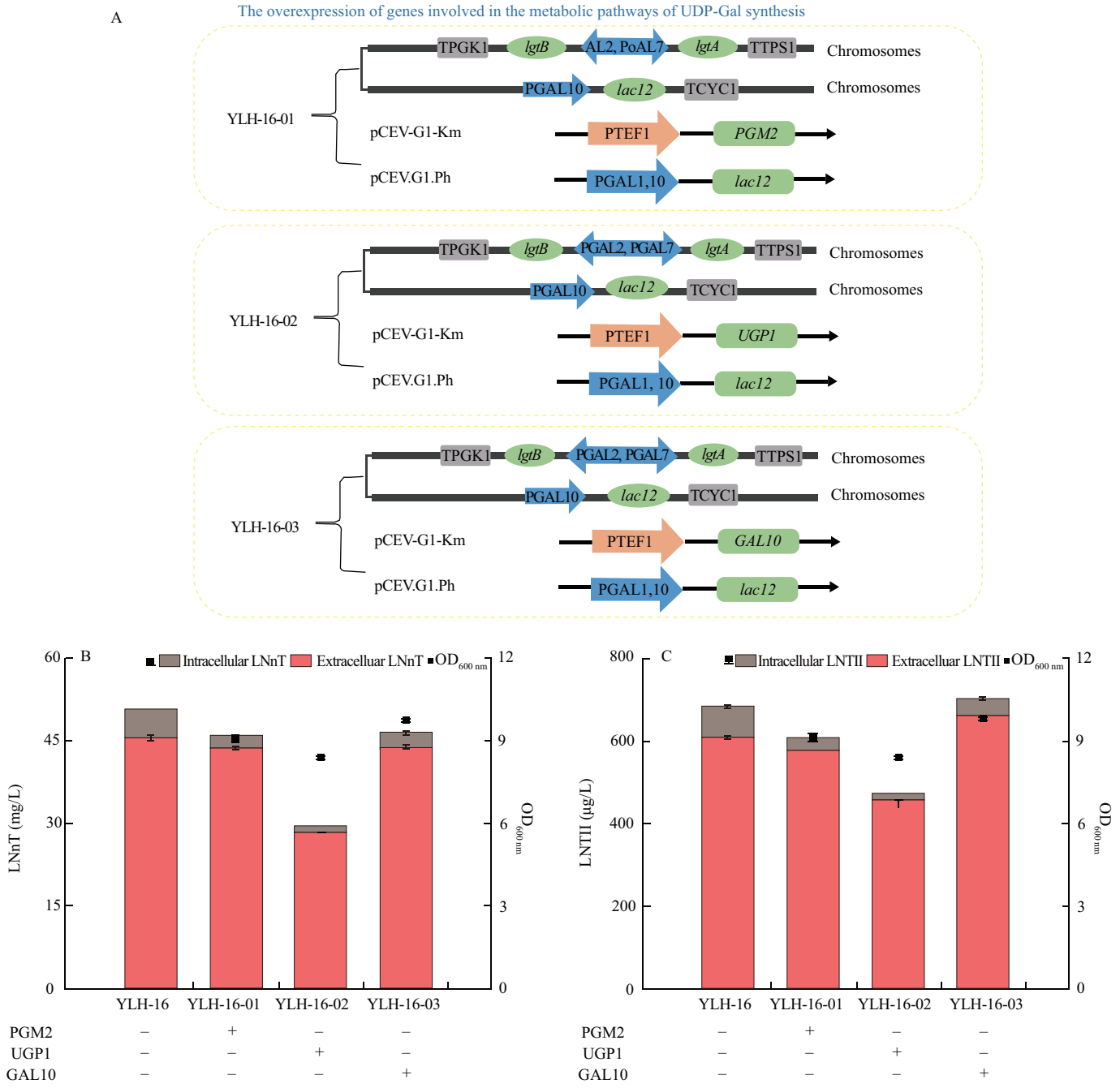

Fig. 8 Comparison of LNnT production in the engineered *S. cerevisiae* with module 2 regulation. (A) *S. cerevisiae* involved in module 2 and their characterization (all strains were based on YLH-11). (B) LC-MS analysis of LNnT synthesis of engineered *S. cerevisiae* YLH-16, YLH-16-01, YLH-16-02, YLH-16-03. (C) LC-MS analysis of LNTII synthesis of the above engineered *S. cerevisiae*. (D) LNnT production and DCW of the above engineered *S. cerevisiae*. (E) LNTII production and DCW of the above engineered *S. cerevisiae*.

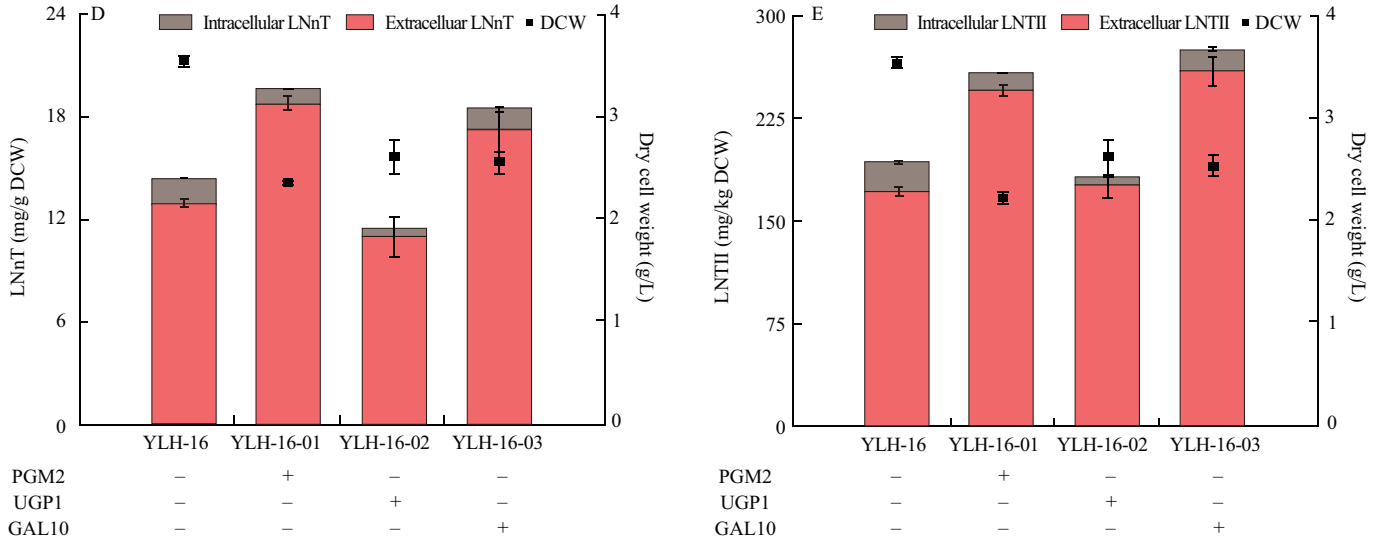

Fig. 8 (*Continued*)

3.3.3 *Module 3-the UDP-GlcNAc supply module*

In module 3, 4 engineered strains (*S. cerevisiae* YLH-16-05, YLH-16-06, YLH-16-07, and YLH-16-08) were constructed by overexpressing the endogenous enzymes GFA1, GNA1, PCM1 and QRI1 in plasmid form within YLH-16 to explore key enzymes of the UDP-GlcNAc supply module (Fig. 9A).

Similar results were obtained for module 2 and module 3. Based on the LNnT and LNTII yields in bar graphs of Figs. 9D and E, the production of *S. cerevisiae* YLH-16-05, YLH-16-06, YLH-16-07 and YLH-16-08 fermentation showed significantly higher yields (LNnT production with 21.37, 16.05, 21.98, and 21.93 mg/g DCW) than that of the parental strain YLH-16 (LNnT production with 14.33 mg/g DCW), which suggests that GFA1, GNA1, PCM1 and QRI1 are key enzymes for module 3. However, the titers of LNnT and LNTII did not show an obvious increase in the engineered strains. It is speculated that although rate-limiting steps exist in module 2 and module 3, the accumulation of LNnT is mainly hindered by the inadequate performance exhibited by the current heterologous enzyme of module 1 rather than module 2/3. In subsequent study, the rate-limiting enzyme genes of module 2 and module 3 will be integrated into the chromosome after the rate-limiting step of module 1, with the aim of enhancing LNnT production.

To further confirm whether the aforementioned enzymes are indeed key endogenous enzymes of module 2 and module 3, chromosomal integration overexpression was performed instead of plasmid overexpression (Fig. 10). And when chromosomal integration was used instead of plasmid overexpression, it was found that the extracellular LNnT titer significantly increased after overexpression of the putative endogenous key enzymes, indicating that the previous speculation was correct and that PGM2, GAL10, GFA1, GNA1, PCM1 and QRI1 are endogenous key enzymes for LNnT synthesis in *S. cerevisiae*. Finally, the LNnT titer in strains YLH-81, YLH-82, YLH-83, YLH-84, YLH-85 and YLH-86 reached 145.56, 121.97, 122.68, 142.48, 140.37 and 145.91 mg/L, respectively.

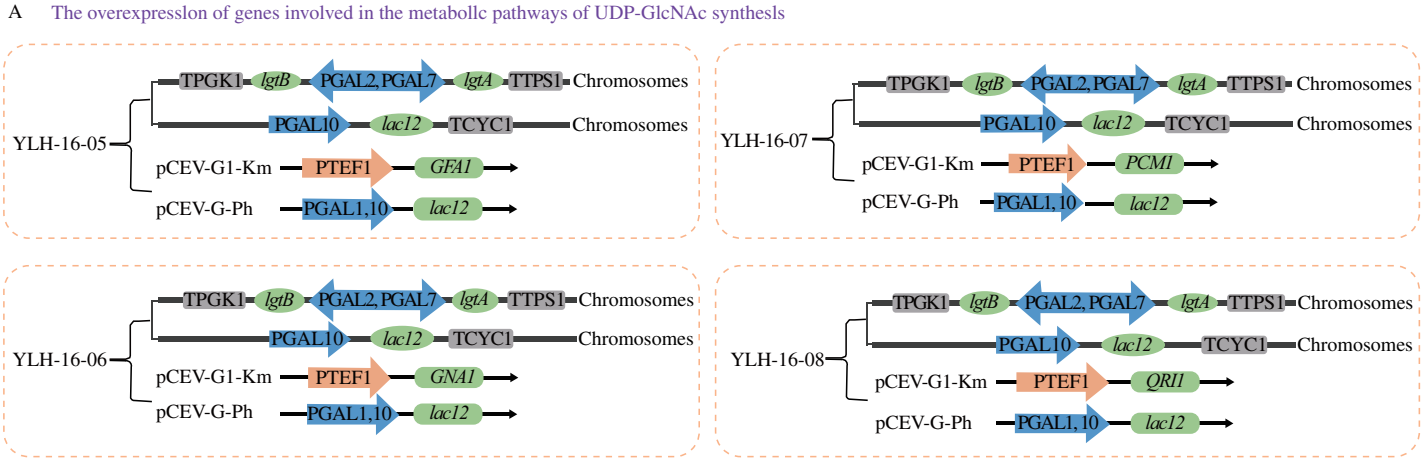

Fig. 9 Comparison of LNnT production in the engineered *S. cerevisiae* in module 3. (A) *S. cerevisiae* involved in module 3 and their characterization (all strains were based on YLH-11). (B) LC-MS analysis of LNnT synthesis of engineered *S. cerevisiae* YLH-16, YLH-16-05, YLH-16-06, YLH-16-07, YLH-16-08. (C) LC-MS analysis of LNTII synthesis of the above engineered *S. cerevisiae*. (D) LNnT production and DCW of the above engineered *S. cerevisiae*. (E) LNTII production and DCW of the above engineered *S. cerevisiae*.

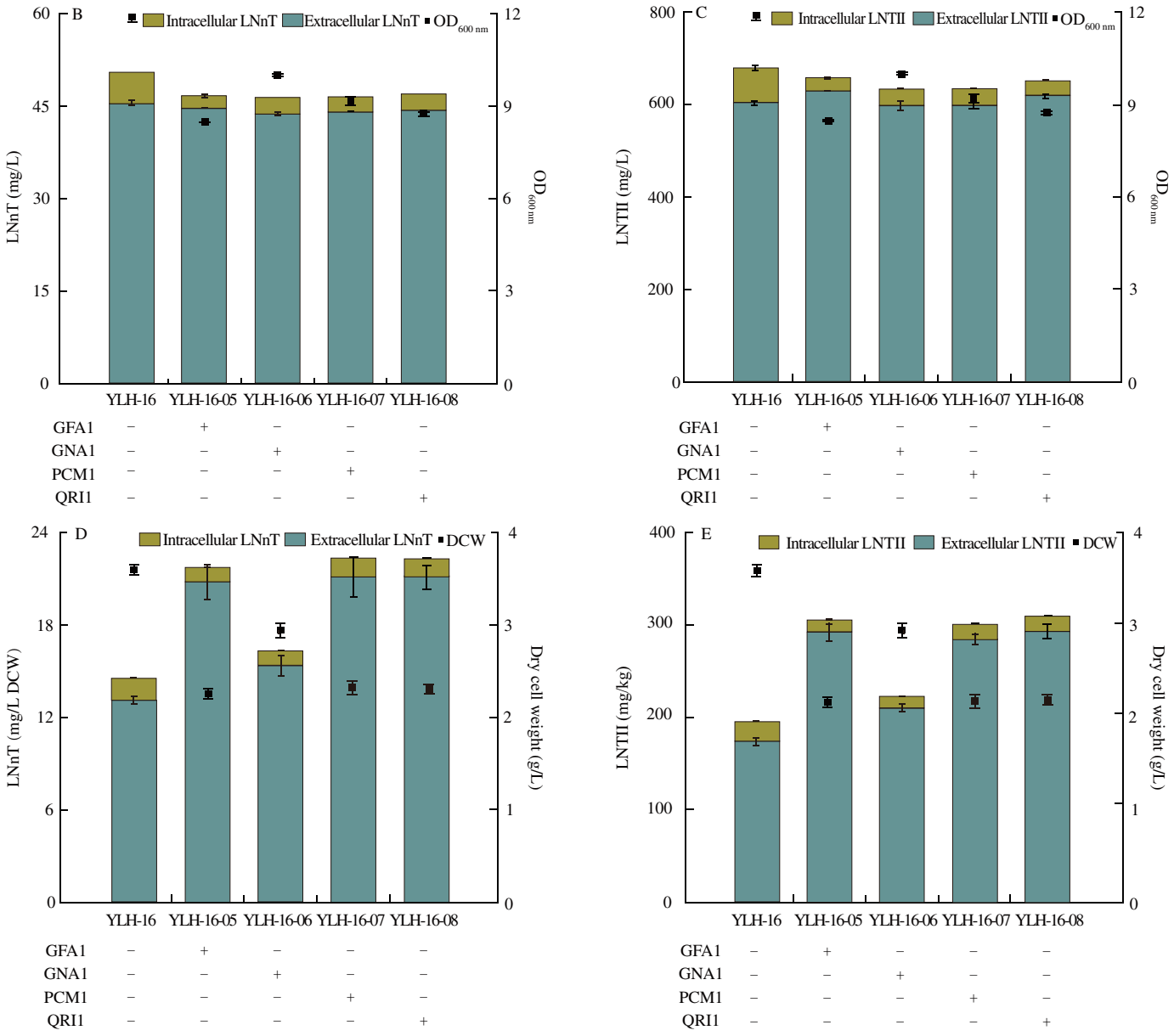

Fig. 9 (*Continued*)

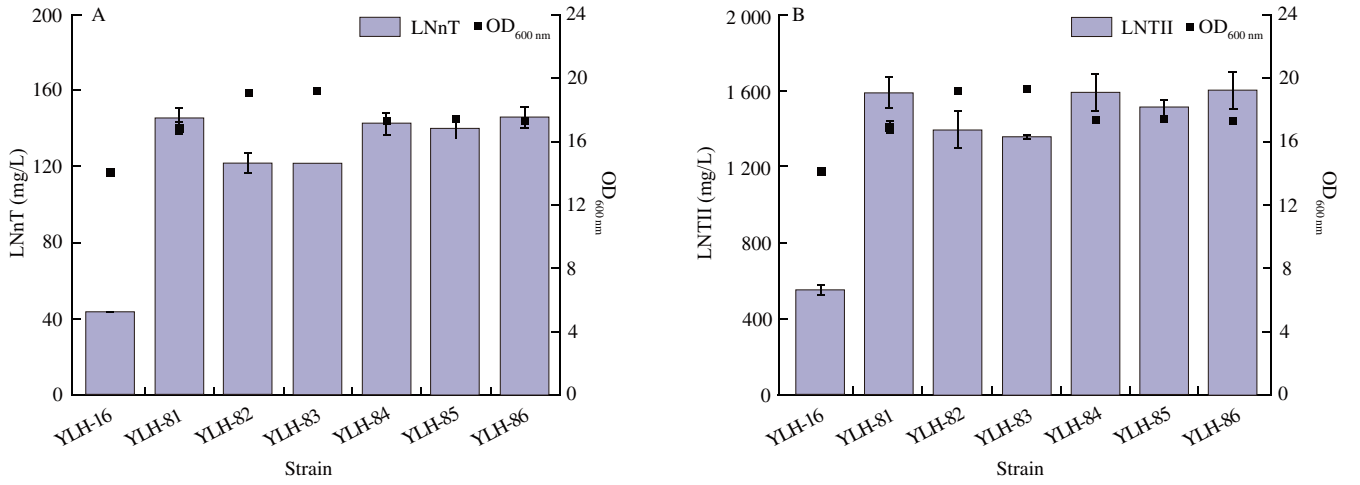

Fig. 10 Validation of endogenous key enzymes by chromosomal integration. (A) LNnT synthesis under key endogenous genes for YLH-16 chromosome integration. (B) LNTII synthesis under key endogenous genes for YLH-16 chromosome integration.

4. Conclusion

In this study, *S. cerevisiae* was successfully engineered for *de novo* synthesis of LNnT. To the best of our knowledge, this is the first report on the LNnT biosynthesis in *S. cerevisiae.* The effect of heterologous gene expression time on LNnT production was verified *via* carbon source regulation based on the GAL regulatory system. Additionally, this study has identified key enzymes for LNnT production, including Lac12, PGM2, GAL10, GFA1, GNA1, PCM1, and QRI1, through multi-module engineering. This work constitutes a cornerstone for *de novo* LNnT synthesis in *S. cerevisiae* and provides helpful information for subsequent research on production improvement.

Nevertheless, a discrepancy persists between the LNnT production capabilities of *Saccharomyces cerevisiae* and those of *E. coli* at this stage. The results of this study indicate that the heterologous genes in module 1 are the primary factors influencing LNnT production, while modules 2 and 3 play a secondary role. Consequently, when overexpressing endogenous genes in plasmid form, the metabolic pressure exerted by the plasmids makes it impossible to effectively screen for key endogenous enzymes according to LNnT titer. In the future, it may be possible to combine key endogenous enzymes from modules 2 and 3 to improve the yield of LNnT after opening up the downstream pathway through screening and enzyme modification.

Acknowledgements

This work was funded by the National Key Research and Development Program of China (2022YFF1100300), National Natural Science Foundation of China (22108097), Key Research and Development Program of Jiangsu Province (BE2022850), Taihu Innovation-Leading Talent of Wuxi City (1026010241230040), Cross-Integration Innovation Funding of SFST (SFST2023-KY-10).

Declaration of competing interest

The authors declare that they have no known competing financial interests or personal relationships that could have appeared to influence the work reported in this paper.

Appendix A. Supplementary data

Supplementary data associated with this article can be found, in the online version, at http://doi.org/10.26599/FSHW.2024.9250342.

References

[1] A.M. Zivkovic, J.B. German, C.B. Lebrilla, et al., Human milk glycobiome and its impact on the infant gastrointestinal microbiota, PNAS 108(Suppl 1) (2011) 4653-4658. https://doi.org/10.1073/pnas.1000083107.

[2] S. Thurl, M. Munzert, J. Henker, et al., Variation of human milk oligosaccharides in relation to milk groups and lactational periods, Br. J. Nutr. 104 (2010) 1261-1271. https://doi.org/10.1017/S0007114510002072.

[3] L. Bode, Human milk oligosaccharides: every baby needs a sugar mama, Glycobiology 22 (2012) 1147-1162. https://doi.org/10.1093/glycob/cws074.

[4] T. Urashima, E. Taufik, K. Fukuda, et al., Recent advances in studies on milk oligosaccharides of cows and other domestic farm animals, Biosci. Biotechnol. Biochem. 77 (2013) 455-466. https://doi.org/10.1271/bbb.120810.

[5] L.L. Xu, S.D. Townsend, Synthesis as an expanding resource in human milk science, J. Am. Chem. Soc. 143 (2021) 11277-11290. https://doi.org/10.1021/jacs.1c05599.

[6] S. Wu, N. Tao, J.B. German, et al., Development of an annotated library of neutral human milk oligosaccharides, J. Proteome Res. 9 (2010) 4138-4151. https://doi.org/10.1021/pr100362f.

[7] J. Zheng, H. Xu, J. Fang, et al., Enzymatic and chemoenzymatic synthesis of human milk oligosaccharides and derivatives, Carbohyd. Polym. 291 (2022). https://doi.org/10.1016/j.carbpol.2022.119564.

[8] B. Farhadihosseinabadi, M. Gholipourmalekabadi, M. Salimi, et al., The *in vivo* effect of lacto-*N*-neotetraose (LNnT) on the expression of type 2 immune response involved genes in the wound healing process, Sci. Rep. 10 (2020) 997. https://doi.org/10.1038/s41598-020-57860-8.

[9] L. Yang, Y. Zhu, J. Meng, et al., Recent progress in fucosylated derivatives of lacto-*N*-tetraose and lacto-*N*-neotetraose, Crit. Rev. Food Sci. Nutr. 64(28) (2024) 0384-10396. https://doi.org/10.1080/10408398.2023.2224431.

[10] K.C. Johnson-Henry, T.R. Abrahamsson, R.Y. Wu, et al., Probiotics, prebiotics, and synbiotics for the prevention of necrotizing enterocolitis, Adv. Nutr. 7 (2016) 928-937. https://doi.org/10.3945/an.116.012237.

[11] B. Hegar, Y. Wibowo, R.W. Basrowi, et al., The role of two human milk oligosaccharides, 2'-fucosyllactose and lacto-*N*-neotetraose, Pediatr. Gastroenterol. Hepatol. Nutr. 22 (2019) 330-340. https://doi.org/10.5223/pghn.2019.22.4.330.

[12] EFSA Panel on Nutrition, A. Food, D. Turck, et al., Safety of the extension of use of 2'-fucosyllactose (2'-FL) and lacto-*N*-neotetraose (LNnT) as novel foods in food supplements for infants pursuant to Regulation (EU) 2015/2283, EFSA J. 20 (2022) e07257. https://doi.org/10.2903/j.efsa.2022.7257.

[13] S. Gallier, K. Vocking, J.A. Post, et al., A novel infant milk formula concept: mimicking the human milk fat globule structure, Colloids Surf. B Biointerfaces 136 (2015) 329-339. https://doi.org/10.1016/j.colsurfb.2015.09.024.

[14] E. Perez-Escalante, S. Alatorre-Santamaria, A. Castaneda-Ovando, et al., Human milk oligosaccharides as bioactive compounds in infant formula: recent advances and trends in synthetic methods, Crit. Rev. Food Sci. Nutr. 62 (2022) 181-214. https://doi.org/10.1080/10408398.2020.1813683.

[15] C.H. Hsu, K.C. Chu, Y.S. Lin, et al., Highly alpha-selective sialyl phosphate donors for efficient preparation of natural sialosides, Chemistry 16 (2010) 1754-1760. https://doi.org/10.1002/chem.200903035.

[16] B. Zeuner, M. Vuillemin, J. Holck, et al., Loop engineering of an alpha-1,3/4-l-fucosidase for improved synthesis of human milk oligosaccharides, Enzyme Microb. Technol. 115 (2018) 37-44. https://doi.org/10.1016/j.enzmictec.2018.04.008.

[17] W. Zhang, Z. Liu, M. Gong, et al., Metabolic engineering of *Escherichia coli* for the production of lacto-*N*-neotetraose (LNnT), Systems Microbiology and Biomanufacturing 1 (2021) 291-301. https://doi.org/10.1007/s43393-021-00023-1.

[18] P. Zhang, Y. Zhu, Z. Li, et al., Designing a highly efficient biosynthetic route for lacto-*N*-neotetraose production in *Escherichia coli*, J. Agric. Food Chem. 70 (2022) 9961-9968. https://doi.org/10.1021/acs.jafc.2c04416.

[19] M. Hu, M. Li, C. Li, et al., High-level productivity of lacto-*N*-neotetraose in *Escherichia coli* by systematic metabolic engineering, J. Agric. Food Chem. 71(9) (2023) 4051-4058 https://doi.org/10.1021/acs.jafc.2c08772.

[20] Y. Liao, J. Wu, Z. Li, et al., Metabolic engineering of *Escherichia coli* for high-level production of lacto-*N*-neotetraose and lacto-*N*-tetraose, J. Agric. Food Chem. 71 (2023) 11555-11566. https://doi.org/10.1021/acs.jafc.3c02997.

[21] B. Priem, M. Gilbert, W.W. Wakarchuk, et al., A new fermentation process allows large-scale production of human milk oligosaccharides by metabolically engineered bacteria, Glycobiology 12 (2002) 235-240. https://doi.org/10.1093/glycob/12.4.235.

[22] X.M. Dong, N. Li, Z.M. Liu, et al., CRISPRi-guided multiplexed fine-tuning of metabolic flux for enhanced lacto-*N*-neotetraose production in *Bacillus subtilis*, J. Agric. Food Chem. 68 (2020) 2477-2484. https://doi.org/10.1021/acs.jafc.9b07642.

[23] X. Dong, N. Li, Z. Liu, et al., Modular pathway engineering of key precursor supply pathways for lacto-*N*-neotetraose production in *Bacillus subtilis*, Biotechn. Biofuels 12 (2019) 212. https://doi.org/10.1186/s13068-019-1551-3.

[24] X. Lv, F. Wang, P. Zhou, et al., Dual regulation of cytoplasmic and mitochondrial acetyl-CoA utilization for improved isoprene production in *Saccharomyces cerevisiae*, Nat. Commun. 7 (2016) 12851. https://doi.org/10.1038/ncomms12851.

[25] P. Yi, N. Li, J.B. Wan, et al., Structural characterization and antioxidant activity of a heteropolysaccharide from *Ganoderma capense*, Carbohydr. Polym. 121 (2015) 183-189. https://doi.org/10.1016/j.carbpol.2014.11.034.

[26] L. Yuan, Z.C. Zhong, Y. Liu, Structural characterisation and immunomodulatory activity of a neutral polysaccharide from *Sambucus adnata* Wall, Int. J. Biol. Macromol. 154 (2020) 1400-1407. https://doi.org/10.1016/j.ijbiomac.2019.11.021.

[27] W. Xie, M. Liu, X. Lv, et al., Construction of a controllable *β*-carotene biosynthetic pathway by decentralized assembly strategy in *Saccharomyces cerevisiae*, Biotechnol Bioeng. 111 (2014) 125-133. https://doi.org/10.1002/bit.25002.

[28] P.J. Westfall, D.J. Pitera, J.R. Lenihan, et al., Production of amorphadiene in yeast, and its conversion to dihydroartemisinic acid, precursor to the antimalarial agent artemisinin, PNAS 109 (2012) E111-118. https://doi.org/10.1073/pnas.1110740109.

[29] P. Zhou, L. Ye, W. Xie, et al., Highly efficient biosynthesis of astaxanthin in *Saccharomyces cerevisiae* by integration and tuning of algal crtZ and bkt, Appl. Microbiol. Biotechnol. 99 (2015) 8419-8428. https://doi.org/10.1007/s00253-015-6791-y.

[30] W. Xie, X. Lv, L. Ye, et al., Construction of lycopene-overproducing *Saccharomyces cerevisiae* by combining directed evolution and metabolic engineering, Metab. Eng. 30 (2015) 69-78. https://doi.org/10.1016/j.ymben.2015.04.0097.

[31] C.B. Brachmann, A. Davies, G.J. Cost, et al., Designer deletion strains derived from *Saccharomyces cerevisiae* S288C: a useful set of strains and plasmids for PCR-mediated gene disruption and other applications, Yeast 14 (1998) 115-132. https://doi.org/10.1002/(SICI)1097-0061(19980130)14:2<115::AID-YEA204>3.0.CO;2-2.